



A Compact Dual-Band CPW-Fed Slot Monopole Antenna for WiFi, WLAN and WiMAX Applications

Omaima Benkhadda¹ · Mohamed Saih¹ · Kebir Chaji¹ · Sarosh Ahmad^{2,3} · Abdelati Reha⁴

Received: 19 April 2022 / Accepted: 30 August 2022 / Published online: 19 September 2022
© King Fahd University of Petroleum & Minerals 2022

Abstract

This article describes the design and manufacturing of a dual-band miniaturized printed monopole antenna for WiFi, wireless local area network and worldwide interoperability for microwave access applications. The developed antenna is constituted of a rectangular radiating element with an elliptical slot printed on a FR-4 substrate and powered by CPW feed technique. The overall area of the designed antenna is $20 \times 35\text{mm}^2$. The dual-band characteristic is achieved by inserting an elliptical slot in the radiator and rectangular and circular slots in the ground plane. To demonstrate the validity of the simulation outcomes, the proposed antenna was fabricated and tested using E5071C VNA, and the experimental outcomes illustrate that the developed antenna provides dual bands: 2.36–2.45 GHz resonating at 2.4 GHz and 3.2–6.29 GHz resonating at 3.8 and 5.5 GHz. Additionally, the recommended antenna has a high peak gain of 3.38 dB and a peak radiation efficiency of 98% percent. Furthermore, the stated design is a suitable applicant for the broadband communication.

Keywords Dual-band · Microstrip patch antenna · CPW-fed · Monopole antenna · WiFi · WLAN · WiMAX

1 Introduction

Over the past few years, a considerable transformation was noted in the field of wireless communication systems. In attempt to support the fast growing of wireless systems, antennas must be able to resonate at a variety of frequencies. As a result, multiband and wideband antennas have been a necessary component of several communication systems including WiFi, wireless local area network (WLAN) and worldwide interoperability for microwave access (WiMAX).

The design tasks assigned to the researchers include the need for an antenna with a planar geometry, easy of manufacturing low profile, low cost, multiband and broadband operations [1]–4. Multiband and dual-band antennas are highly used in wireless communication systems. They permit operation in a variety of frequency bands; hence, they eliminate the need for more separated antennas, thereby attempting to avoid the isolation problem that exists between various antennas.

Various designs for dual-band antennas with rigorous approaches were introduced in [5]–19. The authors in [5] developed a dual-band antenna for WLAN bands, the dual-band characteristic is achieved by introducing several slots in the radiating element. In [6], a multilayer microstrip antenna was introduced for dual-band operation. However, these antennas present narrow bandwidths. A miniaturized dual-band antenna with an artificial magnetic conductor (AMC) surface having an overall size $104 \times 104 \times 3\text{mm}^3$ was designed in [7]. According to [8], a planar antenna with rectangular and circular slots in the ground plane was designed for dual-band operations. In [9], a dual-band PCB monopole antenna was developed. A slotted rectangular antenna was presented in [10] to resonate at two WLAN frequencies: 2.4 and 5.8 GHz. The authors in [11] design a CPW-fed compact antenna consists of a rectangular ring with vertical strips radiator to achieves a dual-band operation. In [12], a dual-band

✉ Omaima Benkhadda
oabekhadda@gmail.com

¹ Microelectronics, Embedded Systems and Telecommunication Team, Faculty of Sciences and Technology, Sultan Moulay Slimane University, 23000 Beni Mellal, Morocco

² Department of Electrical Engineering and Technology, Government College University Faisalabad (GCUF), Faisalabad, Pakistan

³ Department of Signal Theory and Communications, Universidad Carlos III de Madrid, Leganés, 28911 Madrid, Spain

⁴ Laboratory of Innovation in Management and Engineering for the Enterprise (LIMIE), ISGA Marrakech, 40000 Marrakech, Morocco



antenna consists of two pairs of crossed dipoles was introduced for WLAN and WiMAX bands. The authors in [13] developed a dual-band antenna, it consists of slits and rectangular split ring for WLAN applications. In [14], a dielectric resonator MIMO antenna was introduced for dual-band for WLAN and WiMAX applications. In [15], a modified SRR antenna was developed for dual-band operation. An AMC dual-band antenna was developed for WLAN/WBAN applications in [16]. A 4×4 MIMO antenna was introduced to generate a dual-band at 2.4 and 5.8 GHz in [17], it occupies an overall size $66 \times 66 \times 1.6\text{mm}^3$. According to [18], a dual-band planar antenna suitable for WLAN and WiMAX bands was designed, it consists of an U and L-shaped strip radiating element. The authors in [19] proposed a rectangular antenna with dual slot in the radiator to achieve a dual-band for WiFi, WLAN and WiMAX bands. In [20], a dual-band microstrip patch antenna resonating at 2.4 and 5 GHz WLAN bands was designed.

The design described in [21] presents a CP rotated L-shaped antenna for WLAN and V2X bands. According to [22], a C-shaped antenna was designed for WLAN and 5G applications. In [23], a miniaturized flexible decagon ring antenna was proposed for GSM/LTE/5G/WLAN bands. The authors in [24] propose a reconfigurable antenna based on MTM inclusions for 5G applications. In [25], a Hilbert-shaped MTM antenna was designed for RF energy harvesting. An UWB cylindrical MTM antenna was presented in [26] for RF energy harvesting at different the bands of 3.5, 5.8 and 7.5 GHz.

All of the structures of antennas presented above occupy large area, had a narrow bandwidth, or they had a complex structure. Because of all of these considerations, planar antennas ought to have improved performance, including a low profile that enables for multiband characteristic to fulfill the requirements of WiFi, WLAN and WiMAX standards.

The main objective of this article is to develop a miniaturized planar dual-band antenna that can combine WiFi, WLAN and WiMAX communication standards in one device. To obtain simultaneous dual-band operations, the presented antenna consists of rectangular radiator loaded with an elliptical slot powered by a CPW-fed technique. The developed antenna has two bands. The first band ranges from 2.36 to 2.45 GHz, centered at 2.4 GHz, and the second ranges from 3.2 to 6.29 GHz, with two operating frequencies of 3.8 and 5.5 GHz, covering the WiFi, WLAN and WiMAX bands. The first band is created by etching an elliptical slot in the radiator. While, the second band is achieved by utilizing the slots in the ground plane. At the resonant frequencies 2.4/3.8/5.5 GHz, the developed antenna has a good gain and high radiation efficiency of about 15/1.8/3.38 dB and 94/96/98%, respectively. It also has an omnidirectional E- and the H-planes radiation pattern. The remainder of this article is divided into different sections: the first section details the antenna construction

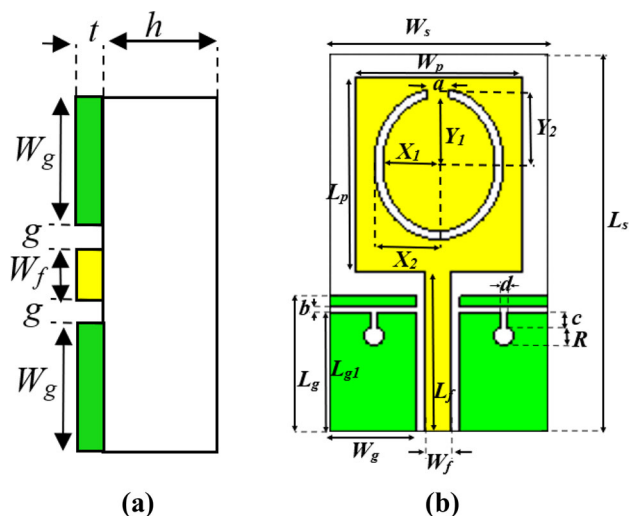


Fig. 1 Geometrical structure of the developed antenna: **a**, side layer; **b**, top layer

methodology. Section 2 displays a parametric study of the developed antenna dimensions. In Sect. 3, the simulation and experimental results are discussed. The work's conclusion is presented in the final section.

2 Antenna Design

2.1 Geometry of the Miniaturized Dual-Band Antenna

The structure of the developed miniaturized planar dual-band antenna is illustrated in Fig. 1. The antenna is constituted of a rectangular radiator with an elliptical slot engraved on the top layer of a 1.6 mm thick FR-4 substrate ($\epsilon_r = 4.4$ and $\tan\delta = 0.002$). And it is powered by a CPW feed line of width 2.4 mm and a gap of 0.8 mm. The ground plane has a rectangular shape loaded by circular and rectangular slots. The proposed antenna has an overall size $20 \times 35\text{mm}^2$. The antenna's dimensions were carefully chosen and optimized using CST MWS, and the dimensions values of the designed antenna as marked in Fig. 1 are: $W_s = 20$ mm; $L_s = 35$ mm; $h = 1.6$ mm; $W_p = 15.5$ mm; $L_p = 18$ mm; $W_f = 2.4$ mm; $L_f = 14.8$ mm; $L_g = 12.5$ mm; $L_{g1} = 11$ mm; $W_g = 8$ mm; $g = 0.8$ mm; $t = 0.035$ mm; $X_1 = 6$ mm; $Y_1 = 7$ mm; $X_2 = 5.2$ mm; $Y_2 = 6.2$ mm; $a = 2$ mm; $b = 0.5$ mm; $c = 1.5$ mm; $d = 0.5$ mm; $R = 1.8$ mm. The developed antenna's process design analysis is displayed in the next section.

2.2 Design Procedure of the Miniaturized Dual-Band Antenna

This section displays and discusses the design procedure of the developed antenna. The use of the elliptical slots and the

Fig.2 Design procedure of the developed dual-band antenna **a**, Antenna 1; **b**, Antenna 2; **c**, Antenna 3; **d**, Antenna 4

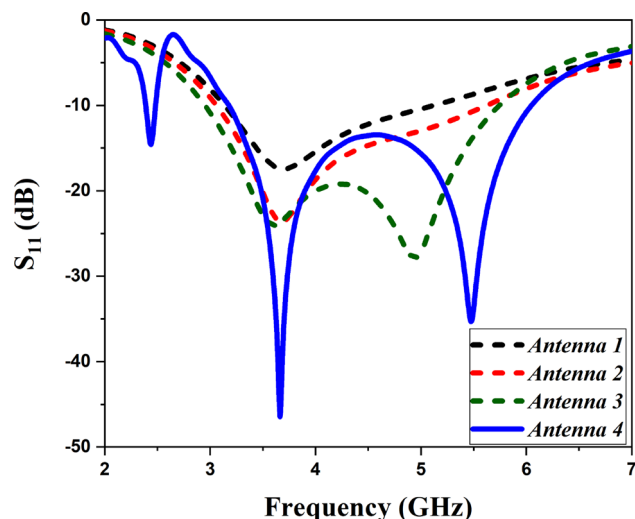
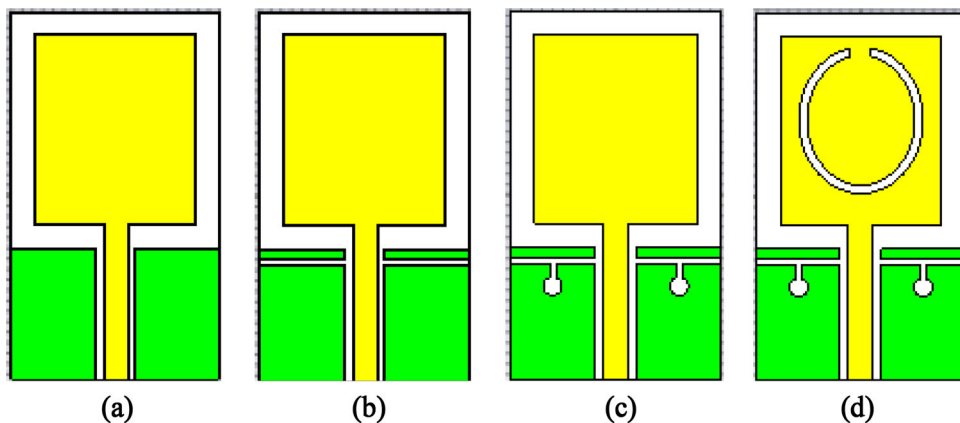


Fig.3 Simulated reflection coefficient S_{11} for several design phases

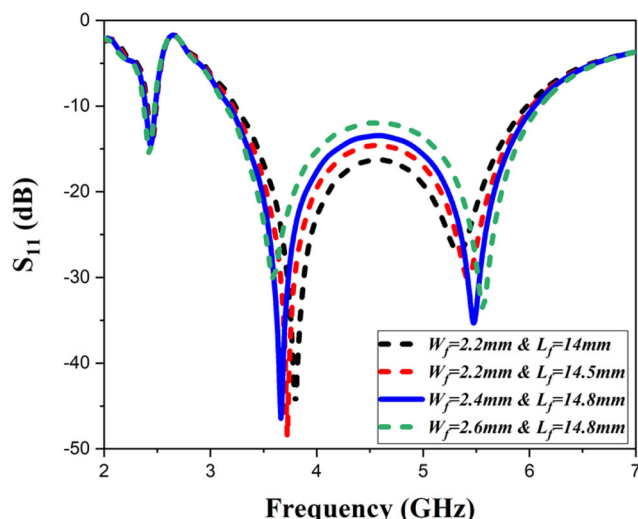


Fig.4 Simulated S_{11} for various values of W_f and L_f

slots incorporated in the ground plane all contribute to obtain the required dual-band. Figure 2 shows the several design phases applied to arrive at the final proposed structure. And the simulated reflection coefficient S_{11} of the several phases of the suggested antenna’s design procedure is exhibited in Fig. 3.

Figure 2a depicts the first phase in the design of the developed antenna. A rectangular radiator powered by a CPW feed line was employed as a reference antenna (antenna 1). The rectangular radiator width W_p and length L_p were calculated by the help of the theory of transmission lines [27, 28]. The width of the radiator W_p can be determined by:

$$W_p = \frac{c}{2f_r} \sqrt{\frac{2}{\epsilon_r + 1}} \tag{1}$$

where c, f_r and ϵ_r are the speed of light in free space, the resonant frequency and relative permittivity, respectively, and

the radiator length L_p is given by Eq. 2:

$$L_p = \frac{c}{2f_r \sqrt{\epsilon_{eff}}} - 2\Delta L_p \tag{2}$$

where ϵ_{eff} and ΔL_p are the effective dielectric constant of the substrate and the normalized length extension due to fringing effects, respectively, and are calculated by Eqs. 3 and 4:

$$\epsilon_{reff} = \frac{\epsilon_r + 1}{2} + \frac{\epsilon_r - 1}{2} \times \left[1 + 12 \frac{h}{W_p} \right]^{-1/2} \tag{3}$$

$$\Delta L = 0, 412 \times h \times \frac{(\epsilon_{reff} + 0, 3) + (\frac{W}{h} + 0, 264)}{(\epsilon_{reff} - 0, 258) + (\frac{W}{h} + 0, 8)} \tag{4}$$

It can be claimed from Fig. 3 that Antenna 1 resonates at 3.6 GHz, and it shields a bandwidth 3.4–4.59 GHz.

For increase the bandwidth rectangular slots of width and length W_g and b , respectively, are inserted in the ground plane (Antenna 2) as presented in Fig. 2b. It can be claimed

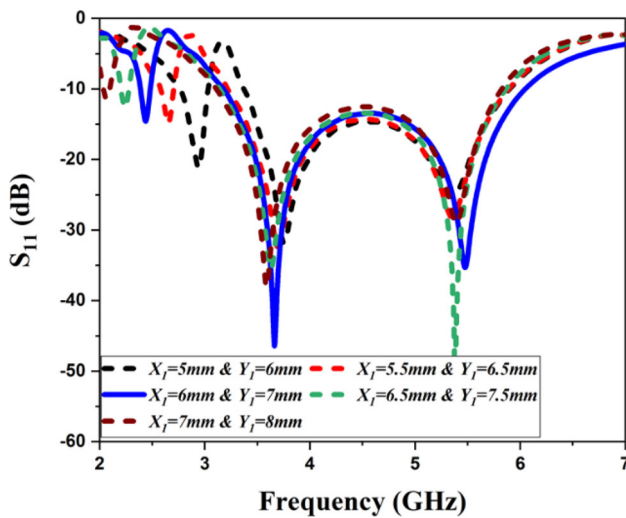


Fig. 5 Simulated S_{11} for various values of X_1 and Y_1

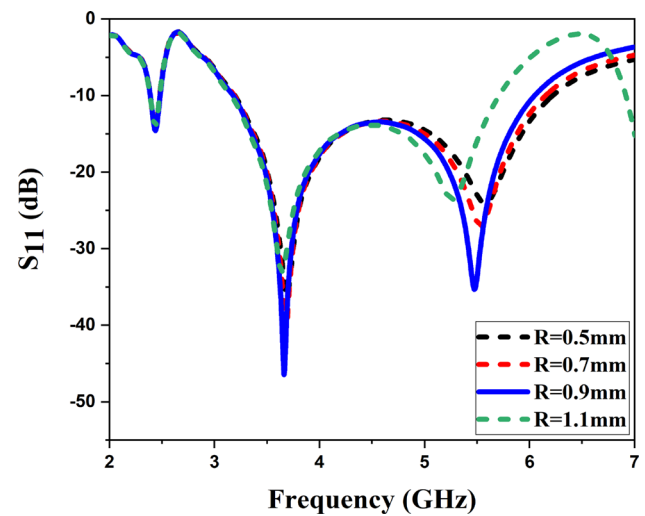


Fig. 8 Simulated S_{11} for various values of R

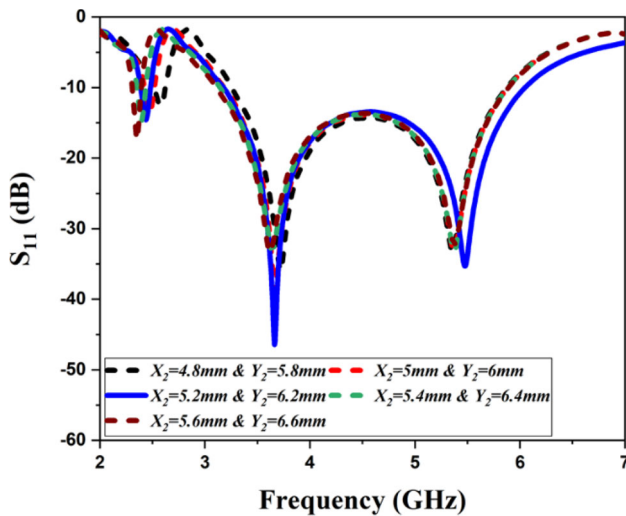


Fig. 6 Simulated S_{11} for various values of X_2 and Y_2

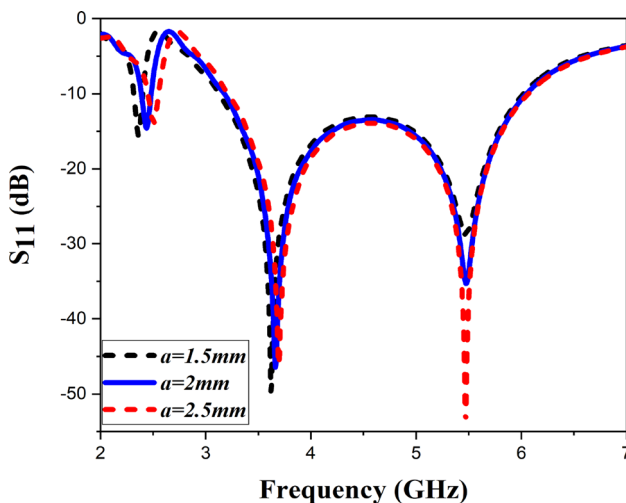


Fig. 7 Simulated S_{11} for various values of a

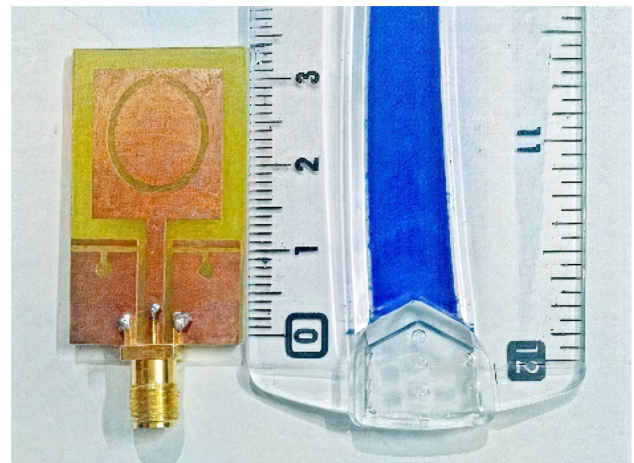


Fig. 9 Manufactured prototype of the developed antenna

from Fig. 3 that Antenna 2 provides an impedance bandwidth from 3.2 GHz to 5.2 GHz while maintaining the resonant frequency at 3.6 GHz.

Antenna 3 is obtained by inserting circular slot of diameter R in the ground plane as illustrated in Fig. 2c. It can be noticed that antenna 3 has two operating frequencies 3.6 GHz and 5.1 GHz with a bandwidth 3–5.4 GHz.

Finally, the structure of the developed antenna is achieved by introducing an elliptical slot in the radiator (Antenna 4), this novel structure allows to achieve two bands 2.35–2.45 GHz and 3.2–6.29 GHz. The current distribution is perturbed by inserting an elliptical slot in the rectangular radiator, which yields the creation of a novel band around 2.4 GHz and enhance the impedance bandwidth of the second band.

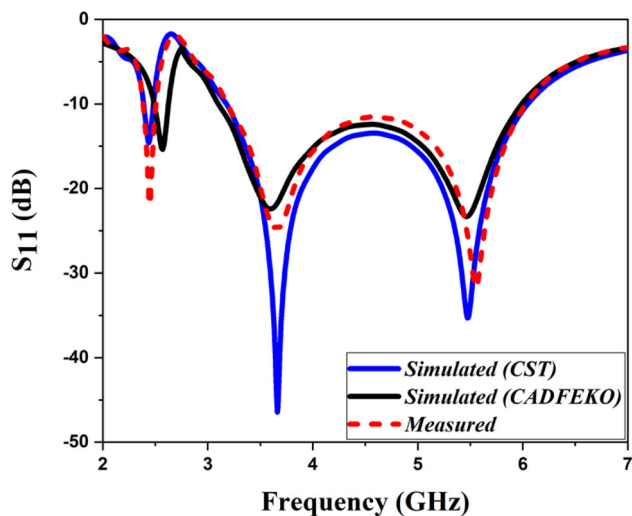


Fig. 10 Measured and simulated reflection coefficient S_{11}

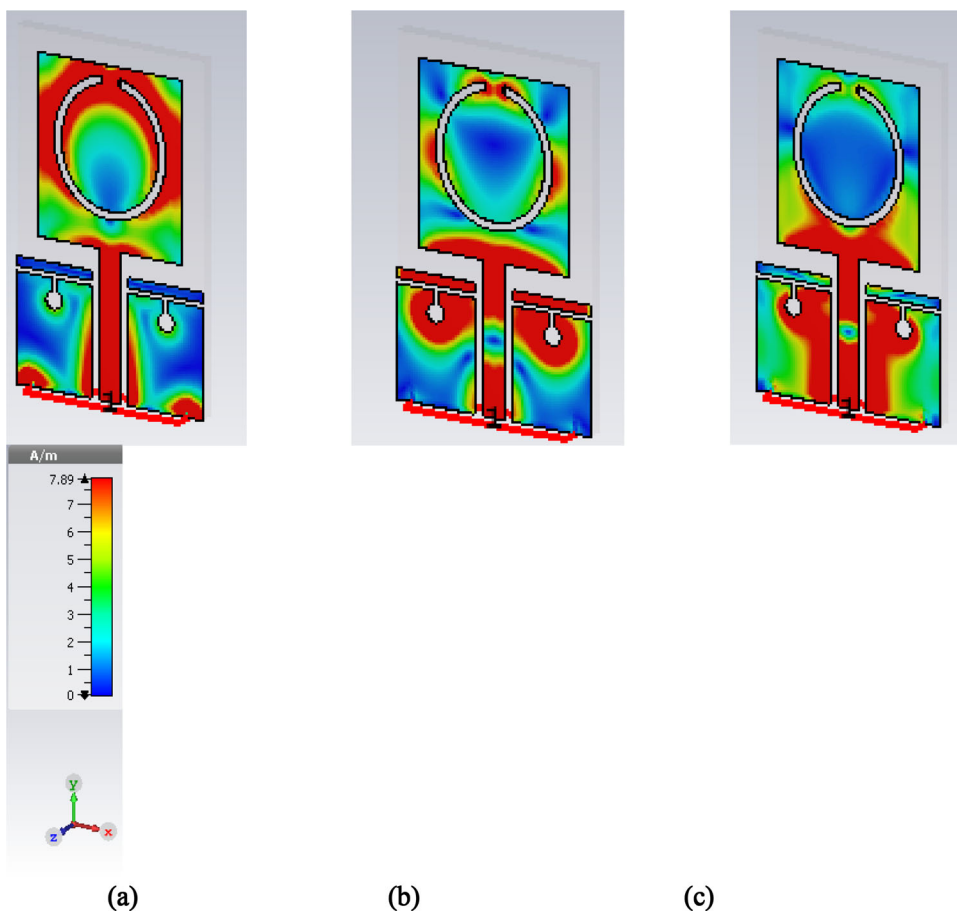
3 Parametric Study

The developed antenna is characterized by its dual operating bands of 2.35–2.45 GHz and 3.2–6.29 GHz. To better understand the influences of antenna parameters on performance, a parametric study was conducted.

Figure 4 depicts the simulated reflection coefficient S_{11} with various values of feed line width and length W_f and L_f . The increment in W_f and L_f enhance the impedance bandwidth of the second band from 2.15 GHz (3.55–5.7 GHz) to 3.09 GHz (3.2–6.29 GHz), while the first band remains unchanged as the feedline width and length varies. Additionally, it can be seen that the optimal value of W_f and L_f are 2.4 mm and 14.8 mm, respectively.

Figure 5 illustrates the effect of X_I and Y_I on the S_{11} , it can be observed from the figure. The values of X_I and Y_I have a significant influence on the first operating frequency. Furthermore, increasing the values of X_I and Y_I shifts the first resonant frequency from 2.1 GHz to 2.85 GHz, and increase the impedance bandwidth of the second operating band from 2.2 GHz (3.5–5.7 GHz) to 3.09 GHz (3.2–6.29 GHz). According to the figure, the values $X_I = 6$ mm and $Y_I =$

Fig. 11 Surface current distribution at a, 2.4 GHz; b, 3.8 GHz; c, 5.5 GHz



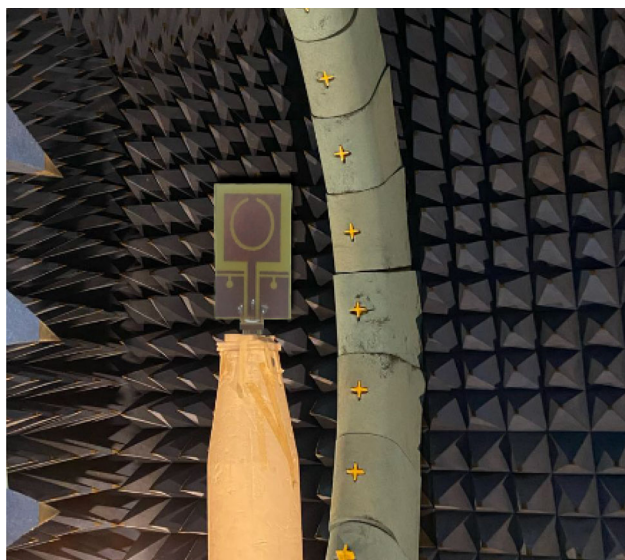


Fig. 12 Measurement setup of the radiation pattern and peak gain

7 mm provide the best performance in terms of bandwidth and impedance matching.

Figure 6 depicts the effect of X_2 and Y_2 on the impedance bandwidth. The increase in X_2 and Y_2 from 4.8 to 5.6 mm and from 6.6 to 5.8 mm, respectively, shifts the first operating frequency from 2.2 to 2.6 GHz, and it improves the impedance bandwidth of the second operating band from 2.6 GHz (3–5.6 GHz) to 3.09 GHz (3.2–6.29 GHz). The optimum values of X_2 and Y_2 are 5.2 mm and 6.2 mm, respectively.

The simulated S_{11} with varied values of a is shown in Fig. 7. The increase in a shifts the first operating frequency from 2.3 to 2.6 GHz, while the second and third operating frequencies remain unchanged with the variation of a . It can be demonstrated that $a = 2$ mm can provide a greater S_{11} value.

Similar to W_f , L_f , X_1 , Y_1 , X_2 , Y_2 and a , R is also varied, as illustrated in Fig. 8. By varying the diameter R from 0.5 to 1.1 mm, the impedance bandwidth decreases from 3.09 GHz

Fig. 13 E-plane radiation pattern at: a, 2.4 GHz; b, 3.8 GHz; c, 5.5 GHz

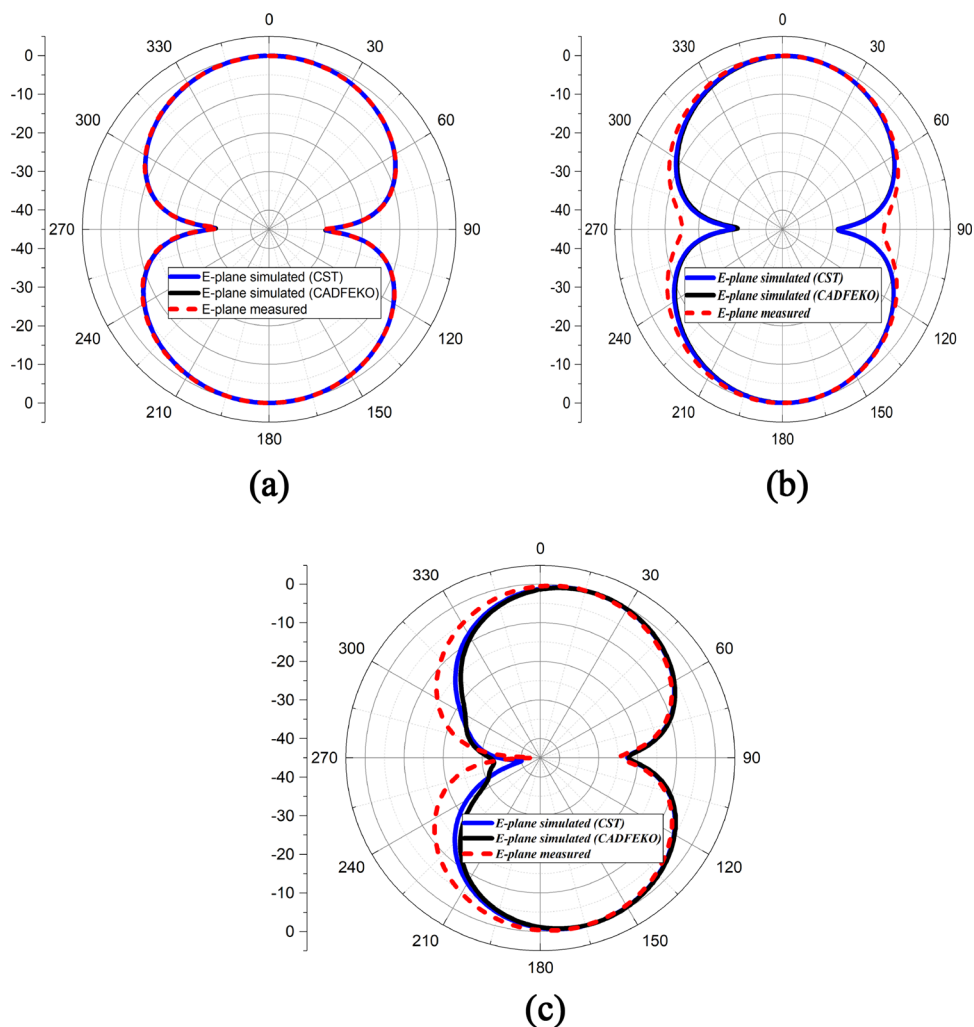


Fig. 14 H-plane radiation pattern at: **a**, 2.4 GHz; **b**, 3.8 GHz; **c**, 5.5 GHz

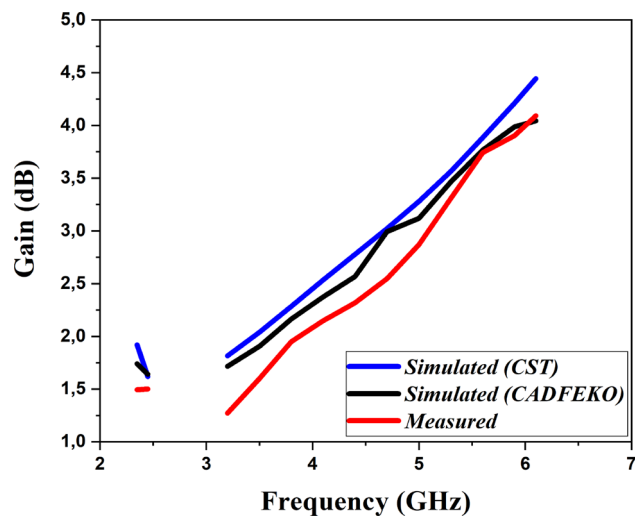
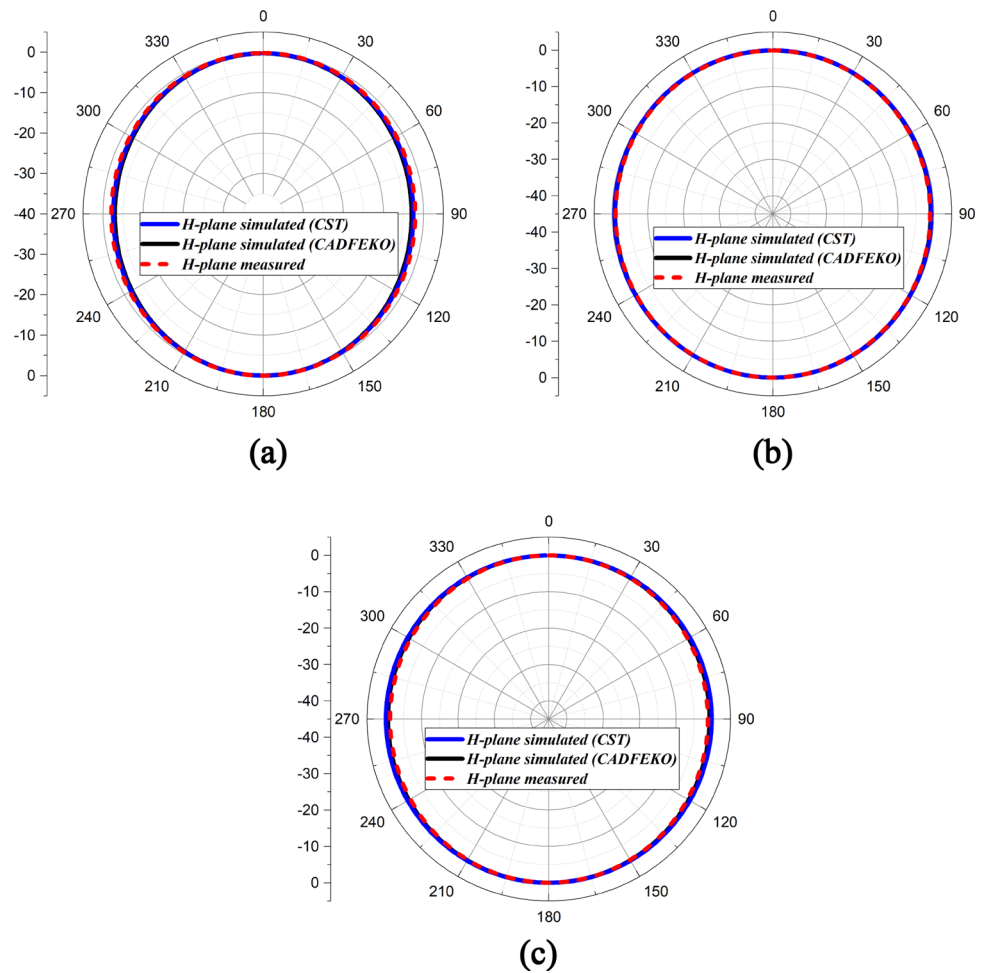


Fig. 15 Measured and simulated gain of the developed antenna

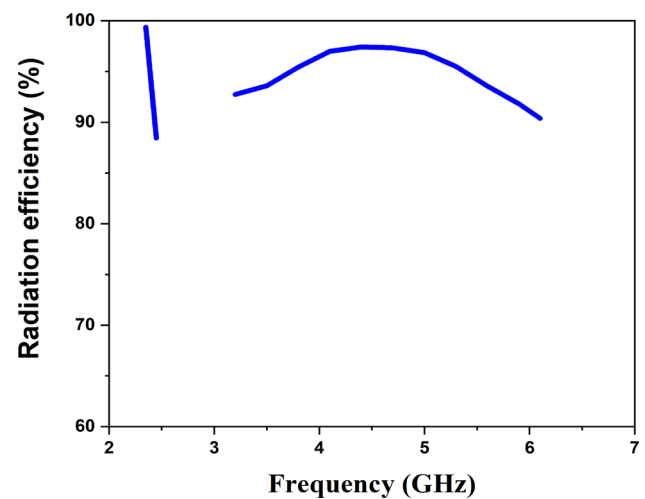


Fig. 16 Simulated radiation efficiency of the developed antenna

(3.2–6.29 GHz) to 2.7 GHz (3.2–5.9 GHz) and the third resonant frequency shifts from 5.7 to 5.4 GHz. Besides, it can

be claimed from the figure that the optimal value of diameter is $R = 0.9$ mm, for which the developed antenna obtains the required dual-band while maintaining good impedance matching.

Table 1 Summary of simulation and measurement results

	CST	FEKO	Measurement
f_r (GHz)	2.4; 3.8; 5.5	2.5; 3.7; 5.54	2.4; 3.75; 5.6
S_{11} (dB)	-15; -47; -37	-16.1; -23.5; -28.4	-22; -25; -32
Bandwidth (MHz)	100; 3020	110; 3015	95; 3021
Gain (dB)	1.8; 2.25; 3.6	1.7; 2.03; 3.43	1.5; 1.8; 3.38

Table 2 Performance comparison of the developed antenna with other dual-band antennas reported in the literature

References	Size(mm ²)	f_r (GHz)	Operating bands (GHz)	Gain (dB)
[5]	20 × 40	2.45; 5.8	(2.37–2.42); (5.7–5.84)	0.4; -1.6
[6]	30 × 30	2.48; 5.9	(2.43–2.52); (5.7–6.5)	6.6; 6
[7]	104 × 104	2.4; 5.2	(2.36–2.76); (5.12–5.62)	7.2; 7.3
[8]	29 × 29	2.4; 5.5	(2.25–2.45); (5.2–5.75)	1; 0.26
[9]	60 × 50	2.45; 5.8	(2.4–2.5); (5.725–5.875)	2.2; 2.8
[13]	50 × 50	1.28; 2.43	(1.198–1.345); (2.395–2.484)	NA
[14]	80 × 80	3.63; 5.05	(3.22–3.97); (4.95–5.51)	5.2; 5.5
[16]	85.5 × 85.5	1.575; 2.45	(1.455–1.965); (2.26–2.57)	1.08; 1.97
[17]	66 × 66	2.4; 5.8	(2.4–2.484); (5.725–5.875)	4; 5.5
[18]	35 × 50	2.5; 5.5	(2.15–3.03); (5–6.05)	2.5; 2.75
[19]	29 × 40	3.5; 5.2	(3.35–3.9); (4.8–6)	NA
[21]	30 × 30	5.5	(4.80–5.99)	2.5
[22]	20 × 15	3.9	(3.3–7.35)	2.25
[24]	62 × 40	3.9; 4.9	–	3; 3.5
[25]	28 × 32	5.8; 8	–	4.5; 7.38
[26]	32 × 15	3; 5.8; 7.5	–	1.2; 2.8; 4
Proposed	20 × 35	2.4; 3.8; 5.5	(2.36–2.45); (3.2–6.29)	1.5; 1.8; 3.38

4 Results and Analysis

To prove the validity of the simulations results acquired by FEKO and CST MWS, the developed antenna is manufactured using FR-4 substrate and Fig. 9 illustrates its prototype. The antenna's S_{11} parameter is measured with an E5071C VNA. Figure 10 exhibits the simulation and experimental outcomes of reflection coefficient S_{11} . The experimental outcomes show that the developed antenna provides two bands 0.095 GHz (2.36–2.45 GHz) and 3.09 GHz (3.2 GHz–6.29 GHz) with three operating frequencies 2.4, 3.8 and 5.5 GHz. The simulation and experimental outcomes show good agreement, confirming the validity of the developed antenna model.

Figure 11 depicts the surface current distributions at 2.4, 3.8 and 5.5 GHz. Figure 11a illustrates that the surface current is highly concentrated surrounding the elliptical slot in the radiator. For 3.8 and 5.5 GHz the current is strongly present around the slots in the ground plane as depicted in Fig. 11b and c. This clarifies the developed antenna's mode of operation.

Figure 12 shows the radiation pattern and peak gain measurement setup. Figures 13 and 14 depict the E- plane and H- plane radiation pattern of the developed antenna at 2.4 GHz, 3.8 GHz and 5.5 GHz, respectively. It can be noticed from the figures that the developed antenna presents an omnidirectional E- and H- planes radiation pattern at the operating frequencies.

Figures 15 and 16 illustrate the variation of gain and the radiation efficiency, respectively. It is important to note that the developed antenna performs excellently in aspects of gain and radiation efficiency. The gain of the developed antenna increased to 1.5 dB for the first band, and the radiation efficiency reached its peak of 97%. In the second band, the gain and radiation efficiency rise to 4.1 dB and 98%, respectively. The designed antenna provides significant gains and radiation efficiencies of 1.5/1.8/3.38 dB and 98/96/94% at operational frequencies of 2.4/3.8/5.5 GHz, respectively.

Table 1 compiles and summarizes the simulation results acquired by FEKO and CST MWS, and the measurement results. It can be claimed from the table that the simulation and measurement results are very close to each other.

Table 2 compares the developed antenna's performance to previously reported antennas in the literature as concerns the size, resonant frequency, impedance bandwidth and gain. The comparison table clearly shows that the developed antenna takes up the least amount of space when compared to other reported antennas. As a result, the designed antenna outperforms some other reported antennas in terms of miniaturization and bandwidth.

5 Conclusion

In this work, a novel compact dual-band monopole antenna is proposed for WiFi, WLAN and WiMAX bands. The dual-band radiator began as a rectangular patch and was later merged with elliptical slots and the slots in the ground plane to function in the 2.4 GHz band and the 3.8/5.5 GHz band. The measurements illustrate that the developed antenna has sufficient bandwidth to cover all of the desired 2.4 GHz WiFi, 2.4/3.5/5.2 GHz WLAN and 3.8/5.5 GHz WiMAX applications. And at 2.4/3.8/5.5 GHz the measured gains and the radiation efficiencies are 1.5/1.8/3.38 dB and 98/96/94%, respectively. As a result, the developed dual-band antenna is suitable for WiFi, WLAN and WiMAX applications due to its numerous advantages of low profile, simple structure, sufficient bandwidth, omnidirectional radiation pattern, high gain and good radiation efficiency. In the next studies, we hope design a MIMO antenna based on the proposed antenna in this work.

References

- Li, L.; Zhang, X.; Yin, X.; Zhou, L.: A Compact Triple-Band Printed Monopole Antenna for WLAN/WiMAX Applications. *Antennas Wirel. Propag. Lett.* **15**, 1853–1855 (2016). <https://doi.org/10.1109/LAWP.2016.2539358>
- Naresh Kumar, D.: Asymmetric CPW fed miniaturized dual polarized monopole antenna for WLAN/WiMAX applications. *J. Phys. Conf. Ser.* **1451**(1), 012017 (2020). <https://doi.org/10.1088/1742-6596/1451/1/012017>
- Benkhadda, O., et al.: Compact broadband antenna with vicsek fractal slots for WLAN and WiMAX applications. *Appl. Sci.* **12**(3), 1142 (2022). <https://doi.org/10.3390/app12031142>
- Ez-Zaki, F.; Belahrach, H.; Ghammaz, A.: Broadband microstrip antennas with cantor set fractal slots for vehicular communications. *Int. J. Microw. Wireless Technol.* **13**(3), 295–308 (2021). <https://doi.org/10.1017/S1759078720000719>
- Ali, M.S.M.; Rahim, S.K.A.; Sabran, M.I.; Abedian, M.; Eteng, A.; Islam, M.T.: Dual band miniaturized microstrip slot antenna for WLAN applications. *Microw. Opt. Technol. Lett.* **58**(6), 1358–1362 (2016). <https://doi.org/10.1002/mop.29803>
- Behera, S.; Barad, D.: Circular polarized dual-band antenna for WLAN/Wi-MAX application. *Int. J. RF Microw. Comput. Aided Eng.* **27**(1), e21046 (2017). <https://doi.org/10.1002/mmce.21046>
- Zhai, H.; Zhang, K.; Yang, S.; Feng, D.: A low-profile dual-band dual-polarized antenna with an AMC surface for WLAN applications. *Antennas Wirel. Propag. Lett.* **16**, 2692–2695 (2017). <https://doi.org/10.1109/LAWP.2017.2741465>
- Patel, R.; Upadhyaya, T.K.: Compact planar dual band antenna for wlan application. *PIER Lett.* **70**, 89–97 (2017). <https://doi.org/10.2528/PIERL17062704>
- Gowrish, B.; Basu, A.: Analysis and design of a dual-band stepped impedance PCB monopole antenna. *IETE J. Educ.* **58**(1), 29–38 (2017). <https://doi.org/10.1080/09747338.2017.1332495>
- Amjad, O.; Munir, S.W.; İmeci, Ş.T.; Ercan, A.Ö.: Design and implementation of dual band microstrip patch antenna for WLAN energy harvesting system. *Appl. Comput. Electromagn. Soc. J.* **33**, 746–751 (2018)
- Manouare, A.Z.; Ibnyaich, S.; Idrissi, A.E.; Ghammaz, A.: A compact CPW-fed dual-band planar monopole antenna for LTE/2.4-GHz/WiMAX, C-band and HiperLAN/2 applications. *J. Circuit Syst. Comp.* **28**(13), 1950220 (2019). <https://doi.org/10.1142/S0218126619502207>
- Le, T.T.; Tran, H.H.: Dual-band dual-sense circularly polarized antenna based on crossed dipole structure for WLAN/WiMAX applications. *Int J RF Microw Comput Aided Eng* **29**(10), e21866 (2019). <https://doi.org/10.1002/mmce.21866>
- Haque, S.K.M.; Alam, H.: Miniaturized dual-band slot antenna design for GPS, amateur radio and WLAN applications. *Int. J. RF Microw. Comput. Aided Eng.* **30**(4), e22125 (2020). <https://doi.org/10.1002/mmce.22125>
- Dwivedi, A.K.; Sharma, A.; Singh, A.K.; Singh, V.: Design of dual band four port circularly polarized MIMO DRA for WLAN/WiMAX applications. *J. Electromagn. Waves Appl.* **34**(15), 1990–2009 (2020). <https://doi.org/10.1080/09205071.2020.1801522>
- Patel, U.; Upadhyaya, T.K.: Dual band planar antenna for GSM and WIMAX applications with inclusion of modified split ring resonator structure. *PIER Letters* **91**, 1–7 (2020). <https://doi.org/10.2528/PIERL20031907>
- Joshi, R., et al.: Dual-band, dual-sense textile antenna with AMC backing for localization using GPS and WBAN/WLAN. *IEEE Access* **8**, 89468–89478 (2020). <https://doi.org/10.1109/ACCESS.2020.2993371>
- Wong, K.-L.; Chen, C.-J.; Li, W.-Y.: Integrated four low-profile shorted patch dual-band WLAN MIMO antennas for mobile device applications. *IEEE Trans. Antennas Propagat.* **69**(6), 3566–3571 (2021). <https://doi.org/10.1109/TAP.2020.3037797>
- Bag, B.; Biswas, P.; Mondal, R.; Biswas, S.; Sarkar, P.P.: Dual-band dual-sense circularly polarized U- and L-shaped strip monopole antenna for WiMAX/WLAN applications. *J. Electromagnet. Waves Appl.* **33**(18), 2434–2448 (2019). <https://doi.org/10.1080/09205071.2019.1684387>
- Sura, P.R.; Sekhar, M.: Circularly polarized dual band dual slot antenna for WLAN Wi-MAX and Wi-Fi applications. *IETE J. Res.* (2020). <https://doi.org/10.1080/03772063.2020.1871423>
- Acıkaya, F.C.; Yıldırım, B.S.: A dual-band microstrip patch antenna for 2.45/5-GHz WLAN applications. *AEU – Int. J. Electron. Commun.* **141**, 153957 (2021). <https://doi.org/10.1016/j.aeu.2021.153957>
- Kulkarni, J.; Sim, C.-Y.-D.; Poddar, A.K.; Rohde, U.L.; Alharbi, A.G.: A compact circularly polarized rotated L-shaped antenna with J-shaped defected ground structure for WLAN and V2X applications. *Prog. Electromagn. Res. Lett.* **102**, 135–143 (2022). <https://doi.org/10.2528/PIERL22010305>
- Sharad Kulkarni J; Desmond Sim C.-Y.: (2020) “Low-Profile, Multiband & Wideband ‘C-Shape’ Monopole Antenna for 5G and WLAN Applications,” In 2020 International Conference on Radar, Antenna, Microwave, Electronics, and Telecommunications



- (ICRAMET), Tangerang, Indonesia. doi: <https://doi.org/10.1109/ICRAMET51080.2020.9298569>.
23. Kulkarni J.; Alharbi A.G.; Sim C.-Y.-D.; Anguera J.: (2022) “Compact, Multiband, Flexible Decagon Ring Monopole Antenna for GSM/LTE/5G/WLAN Applications,” In 2022 16th European Conference on Antennas and Propagation (EuCAP), Madrid, Spain, Mar. pp. 1–5. doi: <https://doi.org/10.23919/EuCAP53622.2022.9769581>.
 24. Al-Khaylani, H.H.; Elwi, T.A.; Ibrahim, A.A.: A novel miniaturized reconfigurable microstrip antenna based printed metamaterial circuitries for 5G applications. *Prog. Electromagn. Res. C* **120**, 1–10 (2022). <https://doi.org/10.2528/PIERC22021503>
 25. Elwi, T.A.; Al-Saegh, A.M.: Further realization of a flexible metamaterial-based antenna on indium nickel oxide polymerized palm fiber substrates for RF energy harvesting. *Int. J. Microw. Wirel. Technol.* **13**(1), 67–75 (2021). <https://doi.org/10.1017/S1759078720000665>
 26. Elwi, T.A.; Jassim, D.A.; Mohammed, H.H.: Novel miniaturized folded UWB microstrip antenna-based metamaterial for RF energy harvesting. *Int. J. Commun. Syst.* **33**(6), e4305 (2020). <https://doi.org/10.1002/dac.4305>
 27. Balanis, C.A.: *Antenna theory: analysis and design*, 3rd edn. John Wiley, Hoboken, NJ (2005)
 28. James J.R.; Hall P.S.: Éd., *Handbook of microstrip antennas*. London, U.K: P. Peregrinus on behalf of the Institution of Electrical Engineers, 1989.

Springer Nature or its licensor holds exclusive rights to this article under a publishing agreement with the author(s) or other rightsholder(s); author self-archiving of the accepted manuscript version of this article is solely governed by the terms of such publishing agreement and applicable law.

